

The Zermelo-Voronoi Diagram: a Dynamic Partition Problem

Efstathios Bakolas and Panagiotis Tsiotras

Abstract—We consider a Dirichlet-Voronoi like partition problem for a small airplane operating in the horizontal plane in the presence of winds that vary uniformly with time. It is shown that the problem can be interpreted as a Dynamic Voronoi Diagram problem, where the generators are not fixed, but rather they are moving targets to be reached in minimum time. The problem is solved by reducing it to a standard Voronoi Diagram by means of a time-varying coordinate transformation.

I. INTRODUCTION

The concept of “Dirichlet-Voronoi Diagram,” first introduced by Dirichlet in 1850 [1], and subsequently generalized by Voronoi in 1908 [2], has found a large spectrum of applications in different fields, including computer graphics, computer vision, computational geometry, robotics and autonomous agents [3], [4], [5], [6], [7]. A Dirichlet-Voronoi Diagram¹ describes a special partition of a topological space equipped with a generalized distance function, which admits a specific relation between each element of the partition and a given discrete set of points, called the *Voronoi generators*. In particular, each element of the partition, known as the *Dirichlet (or Voronoi) domain*, is associated uniquely with a Voronoi generator, in such a way that a point of the space and a Voronoi generator being both in the interior of the same domain implies that the particular Voronoi generator is the “closest” to this point among all other Voronoi generators [4]. We shall refer to the partition problem of a subspace of the n -dimensional Euclidean space (with respect to the Euclidean distance) as the problem of the *standard Voronoi Diagram* (also known in the literature as the ordinary Voronoi Diagram) and as the *generalized Voronoi Diagram* problem otherwise. A detailed treatment of the Voronoi Diagram problem for a plethora of “distance” functions and topologies can be found in [8], [9] and the references therein.

Generalized Voronoi partition problems that are pertinent to autonomous agent applications, when the agents’ dynamics are taken into account, may not be reducible to generalized Voronoi Diagram problems, for which efficient construction schemes exist in the literature. In this work we deal with a partition problem that cannot be put under the umbrella of the available classes of generalized Voronoi Diagram problems. In particular, we deal with the partition problem for a small airplane operating in the Euclidean plane

in the presence of a known wind velocity field (known as the Zermelo’s navigation problem [10]) with the generalized distance being the minimum time from the agent configuration to the goal destination. We henceforth refer to this partition of the configuration space as the Zermelo-Voronoi Diagram (ZVD).

A special case of the ZVD problem, when the wind is constant, is treated in [11], where the solution of the ZVD problem is associated with a standard Voronoi Diagram by means of a coordinate transformation. The approach presented in [11] is, however, of limited scope since it is based on geometric constructive arguments that apply only to constant wind velocity fields. In this work, we introduce a methodology that generalizes the results of [11] under a framework that may prove powerful for dealing with similar partition problems in the future. In particular, by adopting the interpretation of Zermelo’s problem as a moving target problem [12], we reduce the ZVD problem to a Dynamic Voronoi Diagram problem [8], that is, a Voronoi Diagram where the Voronoi generators are not necessarily fixed, but rather they are moving targets. We solve this Dynamic Voronoi Diagram problem by associating it with a standard Voronoi Diagram by means of a time-varying transformation in the case of a time-varying wind field. Furthermore, we introduce the Dual Zermelo-Voronoi Diagram (DZVD) problem, which leads to a partition problem similar to the ZVD problem, with the difference that the generalized distance of the DZVD problem is the minimum time of the Zermelo navigation problem *from* a Voronoi generator *to* a point in the plane. Since the minimum time of the Zermelo navigation problem is not a symmetric function with respect to the initial and final configurations, the ZVD and the DZVD are not, in general, identical.

The case of a non-stationary *spatially-varying* wind field is more complex and a (semi-)analytic treatment of that problem is doubtful. To the authors’ knowledge, the only available result in the literature that deals with spatially-varying (albeit stationary) wind fields are given in [13], [14], where a purely computational/numerical solutions of the problem is presented.

The rest of the paper is organized as follows. In Section II we formulate the Zermelo-Voronoi Diagram problem, and we subsequently demonstrate that it can be interpreted as a Dynamic Voronoi Diagram in Section III. In Sections IV and V we present a scheme for constructing the ZVD and the DZVD respectively by means of a particular homeomorphism applied to a standard Voronoi Diagram. In Section VI we provide simulation results and finally, we conclude with a summary of remarks in Section VII.

E. Bakolas is a Ph.D. candidate at the School of Aerospace Engineering, Georgia Institute of Technology, Atlanta, GA 30332-0150, USA, Email: gth714d@mail.gatech.edu

P. Tsiotras is a Professor at the School of Aerospace Engineering, Georgia Institute of Technology, Atlanta, GA 30332-0150, USA, Email:tsiotras@gatech.edu

¹Henceforth, we shall use the term “Voronoi Diagram” which is the most common terminology in the literature.

II. PROBLEM FORMULATION

The Zermelo-Voronoi Diagram problem deals with a special partition of the Euclidean plane with respect to a generalized distance function, which is related to a classical minimum-time problem named after the mathematician Zermelo, who was the first to pose and solve this problem [10]. In particular, we consider the minimum-time steering problem for a vehicle whose motion is described by the following equation

$$\dot{x} = u + w(x, t), \quad (1)$$

where $x \triangleq (x, y)^\top \in \mathbb{R}^2$ is the position vector of a reference point of the vehicle, $u \in \mathbb{R}^2$ is the control input and $w \triangleq (\mu, \nu)^\top \in \mathbb{R}^2$ is the velocity vector field induced by the winds. We assume that the state space of the system, denoted as \mathfrak{X} , is some connected subset of \mathbb{R}^2 , and the set of admissible control inputs, denoted as \mathcal{U} , consists of all measurable functions that take values in the closed unit ball. The Zermelo's navigation problem (ZNP) can be formulated as follows.

Problem 1 (ZNP): Given the system described by equation (1) determine the control input $u^* \in \mathcal{U}$ such that

- i) The control u^* minimizes the cost functional $J(u) \triangleq T_f$, where T_f is the free final time.
- ii) The trajectory $x^* : [0, T_f] \mapsto \mathfrak{X}$ generated by the control u^* satisfies the boundary conditions

$$x^*(0) = x_0, \quad x^*(T_f) = x_f. \quad (2)$$

The following proposition follows by virtue of Filippov's theorem on the existence of solutions for minimum-time problems [15, p. 311-317].

Proposition 1: Given two points x_0 and x_f in \mathfrak{X} , the existence of a feasible path from x_0 to x_f implies the existence of a minimum-time path as well.

The solution of Problem 1 is the control $u^*(\theta^*) = (\cos \theta^*, \sin \theta^*)$, where θ^* satisfies the following differential equation [16, pp. 370-373]

$$\dot{\theta}^* = (\mu_x - \nu_y) \cos \theta^* \sin \theta^* + \nu_x \sin^2 \theta^* - \mu_y \cos^2 \theta^*, \quad (3)$$

where $\mu_x, \mu_y, \nu_x, \nu_y$ denote partial derivatives.

Next, we formulate the Zermelo-Voronoi Diagram problem (ZVDP).

Problem 2 (ZVDP): Given the system described by equation (1), a collection of goal destinations $P \triangleq \{p_i \in \mathfrak{X} : i \in \mathcal{I}\}$, where \mathcal{I} is a finite index set, and a transition cost

$$c(x_0, p_i) \triangleq T_f(x_0, p_i), \quad (4)$$

determine a partition $\mathfrak{V} = \{\mathfrak{V}_i : i \in \mathcal{I}\}$ of \mathfrak{X} such that

- i) $\mathfrak{X} = \bigcup_{i \in \mathcal{I}} \mathfrak{V}_i$.
- ii) $\overline{\mathfrak{V}_i} = \mathfrak{V}_i$, for each $i \in \mathcal{I}$.
- iii) for each $x \in \text{int}(\mathfrak{V}_i)$, $c(x, p_i) < c(x, p_j)$ for $j \neq i$.

The set of goal destinations P is known in the literature as the set of *Voronoi generators* or *sites*, whereas the partition \mathfrak{V}

constitutes the *Zermelo-Voronoi Diagram* of \mathfrak{X} . Furthermore, an element \mathfrak{V}_i of \mathfrak{V} is called the *Dirichlet domain* or the *Voronoi cell* or the *Voronoi polygon* of the Zermelo-Voronoi Diagram \mathfrak{V} . Two Dirichlet domains \mathfrak{V}_i and \mathfrak{V}_j are characterized as neighboring if they have a non-empty and non-trivial (a single point) intersection. It follows readily from the formulation of Problem 2 and the basic properties of the standard Voronoi Diagram that a point $x \in \partial \mathfrak{V}_i$ satisfies $c(x, p_i) = c(x, p_j)$ for some $j \in \mathcal{I}$, with $j \neq i$, if \mathfrak{V}_i and \mathfrak{V}_j are neighboring Dirichlet domains. Next, we show that it is possible to associate the ZVDP with a Dynamic Voronoi Diagram problem, that is, a Voronoi-like partition problem in the plane when the Voronoi generators are moving targets, by means of a time-varying transformation.

III. THE ZERMELO-VORONOI DIAGRAM INTERPRETED AS A DYNAMIC VORONOI DIAGRAM

The minimum time of the ZNP does not provide us, in general, with a generalized distance function that would allow us to reduce the ZVDP to a generalized Voronoi Diagram, for the construction of which efficient computational techniques are available [8]. Therefore, we need to adopt an alternative approach.

In order to simplify our discussion we assume that $|w(x, t)| < 1$, which implies complete controllability of the system (1) (see for example [16]). Thus, we will henceforth assume that $\mathfrak{X} = \mathbb{R}^2$. We show that it is possible to associate Problem 2 for the case when $w = w(t)$ with a standard Voronoi Diagram.

Problem 3 (ZNMTP): Given the system described by the equation

$$\dot{X} \triangleq \dot{x} - w(t) = u(t), \quad X(0) = x_0 \quad (5)$$

determine the control input $u^* \in \mathcal{U}$ such that

- i) The control u^* minimizes the cost functional $J(u) \triangleq T_f$, where T_f is the free final time.
- ii) The trajectory $X^* : [0, T_f] \mapsto \mathbb{R}^2$ generated by the control u^* satisfies the boundary conditions

$$X^*(0) = x_0, \quad X^*(T_f) = x_f - \int_0^{T_f} w(\tau) d\tau. \quad (6)$$

It is clear that Problems 1 and 3 are equivalent, in the sense that a solution of Problem 1 is also a solution of Problem 3, and vice versa. Furthermore, an optimal trajectory X^* of Problem 3 is related to an optimal trajectory x^* of Problem 1 by means of the time-varying transformation

$$X^*(t) = x^*(t) - \int_0^t w(\tau) d\tau. \quad (7)$$

By virtue of (3), for $w = w(t)$ the optimal control of Problem 1 is given by $u^* = (\cos \theta^*, \sin \theta^*)$ (x coordinates) where θ^* is a constant. Furthermore, equation (5) implies that the same control u^* is also the optimal control for the moving target Problem 3 (X coordinates). The application of a constant input to the system described by (5) implies that the optimal path in X -coordinates is a straight line segment, and

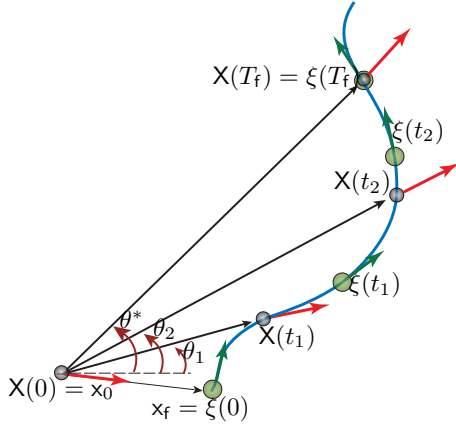


Fig. 1. Time-optimal control strategy for the ZNMTP.

thus the minimum time (invariant under the transformation (7)) is the length of that line segment (since the pursuer moves with constant unit speed the time of motion equals the length of the path). The optimal control strategy for the ZNMTP is depicted in Fig. 1 (constant bearing angle pursuit strategy). In particular, the pursuer (denoted as a black dot) and the moving target (denoted as green dot) start at time $t = 0$ from x_0 and x_f respectively. Since the angle θ^* is necessarily constant, the pursuer is constrained to travel along a line segment that passes through the point x_0 with constant unit speed, whereas the target moves along the time-parameterized curve given by $\xi(t) = x_f - \int_0^t w(\tau) d\tau$. From Proposition 1 it follows that there exists a time $T > 0$ such that $X(T) = \xi(T)$. The optimal value of θ^* corresponds to the least T , denoted as T_f , such that $X(T_f) = \xi(T_f)$. It is easy to show that the minimum time T_f is the least positive root of the following integral-algebraic equation

$$T = |x_f - x_0 - \int_0^T w(\tau) d\tau|, \quad (8)$$

whereas θ^* is given by $\theta^* = \text{Arg} \left((x_f - x_0 - \int_0^{T_f} w(\tau) d\tau) \right)$.

The idea of reducing the ZNP to a moving target problem in the Euclidean plane with no winds (ZNMTP), can also be applied to the ZVDP. In particular, the ZVDP can be formulated as a Dynamic Voronoi Diagram Problem (DVDP).

Problem 4 (DVDP): Given the system described by equations (1), a collection of moving targets $P^d \triangleq \{P_i : P_i(t) = p_i - \int_0^t w(\tau) d\tau, i \in \mathcal{I}\}$, where \mathcal{I} and p_i as in Problem 2, and a transition cost

$$c^d(x_0, P_i) \triangleq |x_0 - P_i(T_f(x_0, p_i))|, \quad (9)$$

determine a partition $V^d = \{V_i^d : i \in \mathcal{I}\}$ of \mathfrak{X} such that

- i) $\mathfrak{X} = \bigcup_{i \in \mathcal{I}} V_i^d$.
- ii) $V_i^d = V_i^d$, for each $i \in \mathcal{I}$.
- iii) for each $x \in \text{int}(V_i^d)$, $c^d(x, P_i) < c^d(x, P_j)$ for $j \neq i$.

Problem 4 deals with the characterization of the sets of initial conditions from which the agent will intercept the moving target set P^d in minimum time. The generalized

distance function is the Euclidean distance between the initial configuration of the agent and the location of the moving target P_i at a specific instant of time, namely, $T_f(x_0, p_i)$, that is, the minimum time of the ZNP from x_0 to $p_i = P_i(0)$. Figure 2 demonstrates the interpretation of the ZVDP as a Dynamic Voronoi Diagram problem. In particular, the target set, which at time $t = 0$ is the set of the Voronoi generators $P = \{p_i, i \in \mathcal{I}\}$ of the ZVDP, moves uniformly with time along the integral curves of the velocity field $-w$.

As we have shown previously, the system (5) with $X(0) = X_0$ reaches a point X_f (not prescribed a priori) in minimum time $T_f = |X_0 - X_f|$. Thus, by reversing time in (7), the system (1) starting at point x'_0 at $t = 0$ reaches the point $x_f = X_f$ in minimum time $T_f = |X_0 - X_f|$, provided that

$$x'_0 = X_0 - \int_0^{d(X_0, X_f)} w(\tau) d\tau, \quad (10)$$

where $d(X_0, X_f) \triangleq |X_0 - X_f|$.

For each Voronoi generator p , equation (10) induces a state transformation $f_p : \mathbb{R}^2 \mapsto \mathbb{R}^2$, where

$$f_p(X) \triangleq X - \int_0^{d(X, p)} w(\tau) d\tau. \quad (11)$$

The following proposition will prove useful for the following discussion.

Proposition 2: Given $p \in \mathbb{R}^2$, the state transformation in (11) is an injective mapping with non-singular Jacobian for all $X \in \mathbb{R}^2$, provided that $|w(t)| < 1$ for all $t \geq 0$.

Proof: First we show that f_p is an injective mapping. Let X_1 and X_2 be such that $f_p(X_1) = f_p(X_2)$, equivalently,

$$X_2 - X_1 = \int_{d(X_2, p)}^{d(X_1, p)} w(\tau) d\tau. \quad (12)$$

By hypothesis $|w(t)| < 1$, and thus (12) gives

$$|X_2 - X_1| \leq |d(X_1, p) - d(X_2, p)|. \quad (13)$$

The injectivity of f_p follows readily in light of the triangle inequality. The Jacobian of f_p at X is equal to

$$Df_p(X) = I_2 - w(d(X, p))(X - p)^T / d(X, p). \quad (14)$$

It can be easily shown that the nonzero eigenvalue of the rank one matrix $w(d(X, p))(X - p)^T / d(X, p)$ is given by

$$\lambda_2(X) = w^T(d(X, p))(X - p) / d(X, p) \leq |w(d(X, p))| < 1.$$

Thus $0 \notin \text{spec}(Df_p(X))$ and the Jacobian $Df_p(X)$ is non-singular for all $X \in \mathbb{R}^2$. ■

The following two propositions follow readily from the previous discussion.

Proposition 3: The coordinates of every element of the set P are invariant under the state transformation (11), that is, $f_p(p) = p$ for all $p \in P$.

Proposition 4: Given $p \in \mathbb{R}^2$, then $c(x, p) = |X - p|$ provided that $x = f_p(X)$.

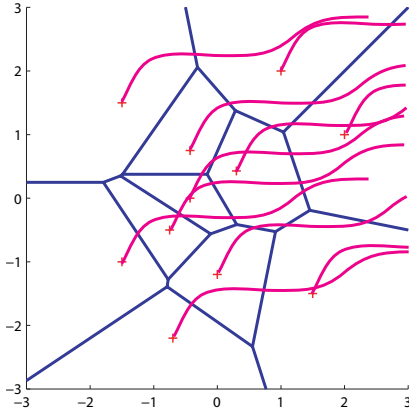


Fig. 2. The Zermelo-Voronoi Diagram can be interpreted as a Dynamic Voronoi Diagram.

IV. CONSTRUCTION OF THE ZERMELO-VORONOI DIAGRAM

In this section, we demonstrate the steps for the construction of the ZVD. In particular, we show that the state transformation (11) reduces the ZVD to a standard Voronoi Diagram for the case of two Voronoi generators. Subsequently, we generalize the previous result to the case of arbitrary finite sets of Voronoi generators.

Let us first consider two distinct points, p_1 and p_2 , in the Euclidean plane. The bisector of p_1 and p_2 is the straight line $\chi(p_1, p_2)$ defined by

$$\begin{aligned} \chi(p_1, p_2) &\triangleq \{X \in \mathbb{R}^2 : |X - p_1| = |X - p_2|\} \\ &= \{X \in \mathbb{R}^2 : (p_2 - p_1)^T X = (|p_2|^2 - |p_1|^2)/2\}. \end{aligned}$$

Correspondingly, the bisector of p_1 and p_2 with respect to the cost (4) is the curve $\gamma(p_1, p_2)$ defined by

$$\gamma(p_1, p_2) \triangleq \{x \in \mathbb{R}^2 : c(x, p_1) = c(x, p_2)\}. \quad (15)$$

The bisector $\chi(p_1, p_2)$ divides \mathbb{R}^2 into the two half-planes $H_1(p_1, p_2) = \{X \in \mathbb{R}^2 : |X - p_1| \leq |X - p_2|\}$ and $H_2(p_1, p_2) = \{X \in \mathbb{R}^2 : |X - p_1| \geq |X - p_2|\}$.

Proposition 5: Given $p_1, p_2 \in \mathbb{R}^2$, and a wind velocity-field w with $|w(t)| < 1$ for all $t \geq 0$, let the function $F : \mathbb{R}^2 \mapsto \mathbb{R}^2$ be defined by

$$F(X) \triangleq \begin{cases} f_{p_1}(X), & X \in H_1(p_1, p_2), \\ f_{p_2}(X), & X \in H_2(p_1, p_2). \end{cases} \quad (16)$$

Then the following statements are true.

- i) The map F is continuous for all $X \in \mathbb{R}^2$ and continuously differentiable for all $X \notin \chi(p_1, p_2)$.
- ii) The sets $F(H_1(p_1, p_2))$ and $F(H_2(p_1, p_2))$ are connected.
- iii) The sets $F(H_1(p_1, p_2))$ and $F(H_2(p_1, p_2))$ are closed, and $\partial F(H_1(p_1, p_2)) = \partial F(H_2(p_1, p_2)) = F(\chi(p_1, p_2))$.
- iv) $\text{int}(F(H_1(p_1, p_2))) \cap \text{int}(F(H_2(p_1, p_2))) = \emptyset$ and $F(H_1(p_1, p_2)) \cap F(H_2(p_1, p_2)) = F(\chi(p_1, p_2))$.
- v) The map F is a homeomorphism.

- vi) $p_1 \in \text{int}(F(H_1(p_1, p_2)))$ and $p_2 \in \text{int}(F(H_2(p_1, p_2)))$.
- vii) For all $x \in \text{int}(F(H_1(p_1, p_2)))$, $c(x, p_1) < c(x, p_2)$. Similarly, for all $x \in \text{int}(F(H_2(p_1, p_2)))$, $c(x, p_2) < c(x, p_1)$.
- viii) The bisector of p_1 and p_2 with respect to the cost c satisfies

$$\gamma(p_1, p_2) = \{x \in \mathbb{R}^2 : x = F(X), X \in \chi(p_1, p_2)\}.$$

Proof:

- i) First, we show that F is well defined for $X \in H_1(p_1, p_2) \cap H_2(p_1, p_2) = \chi(p_1, p_2)$. In particular, for $X \in \chi(p_1, p_2)$, we have that $d(X, p_1) = d(X, p_2)$, which implies that $f_{p_1}(X) = f_{p_2}(X)$. The continuity of F follows readily. Furthermore, the Jacobian of F is well defined and invertible (see Proposition 2) for all $X \in \mathbb{R}^2 \setminus \chi(p_1, p_2)$, and it is given by (??) for X in $H_1(p_1, p_2)$ and $H_2(p_1, p_2)$, respectively.
- ii) It follows immediately from the continuity of F .
- iii) First, notice that the restriction of F on $H_1(p_1, p_2)$, is f_{p_1} which is an injective, continuously differentiable map with non-singular Jacobian (Proposition 2). It follows that f_{p_1} is a diffeomorphism from $H_1(p_1, p_2)$ to $F(H_1(p_1, p_2)) = f_{p_1}(H_1(p_1, p_2))$ and $F(H_1(p_1, p_2))$ is closed since $H_1(p_1, p_2)$ is closed. Furthermore, $\partial F(H_1(p_1, p_2)) = F(\partial H_1(p_1, p_2)) = F(\chi(p_1, p_2))$. The proof for $F(H_2(p_1, p_2))$ is similar.
- iv) Assume, on the contrary, that there exists $y \in \text{int}(F(H_1(p_1, p_2))) \cap \text{int}(F(H_2(p_1, p_2)))$. It follows from iii) that there are points $X_1 \in \text{int}(H_1(p_1, p_2))$ and $X_2 \in \text{int}(H_2(p_1, p_2))$ with $F(X_1) = F(X_2) = y$. Thus $c(F(X_1), p_1) = c(F(X_2), p_1)$ and $c(F(X_1), p_2) = c(F(X_2), p_2)$, which imply, using Proposition 4, that $|X_1 - p_1| = |X_2 - p_1| = \delta_1$ and $|X_1 - p_2| = |X_2 - p_2| = \delta_2$ respectively, for some positive constants δ_1 and δ_2 . Thus X_1 and X_2 lie necessarily at the intersection of two circles centered at p_i and have radii δ_i , $i \in \{1, 2\}$, respectively. This intersection is non-empty if one of the following conditions hold true: a) $\delta_1 < \delta_2$ with $|p_1 - p_2| \leq \delta_1 + \delta_2$, which implies that both X_1 and X_2 are in $H_1(p_1, p_2)$, b) $\delta_1 > \delta_2$ with $|p_1 - p_2| \leq \delta_1 + \delta_2$, which implies that both X_1 and X_2 are in $H_2(p_1, p_2)$ and finally, c) $\delta_1 = \delta_2$ with $|p_1 - p_2| \leq \delta_1 + \delta_2$, which implies that both X_1 and X_2 are in $\chi(p_1, p_2)$. All previous cases contradict the assumption that $X_1 \in \text{int}(H_1(p_1, p_2))$ and $X_2 \in \text{int}(H_2(p_1, p_2))$. The second part of the statement follows readily.
- v) First, we show that F is injective. First, notice that, by definition, F is injective on $H_1(p_1, p_2)$ and $H_2(p_1, p_2)$. Let now $X_1 \in \text{int}(H_1(p_1, p_2))$ and $X_2 \in \text{int}(H_2(p_1, p_2))$ and assume, on the contrary, that $F(X_1) = F(X_2)$. But $F(X_1) \in F(\text{int}(H_1(p_1, p_2))) \subseteq \text{int}(F(H_1(p_1, p_2)))$ since the restriction of F on $H_1(p_1, p_2)$ is an open map. Similarly, $F(X_2) \in F(\text{int}(H_2(p_1, p_2))) \subseteq \text{int}(F(H_2(p_1, p_2)))$. Hence $F(X_1) = F(X_2)$ implies that $\text{int}(F(H_1(p_1, p_2))) \cap \text{int}(F(H_2(p_1, p_2))) \neq \emptyset$, which contradicts iv). Since F is injective it follows readily that its inverse F^{-1}

exists and it is defined by

$$F^{-1}(x) \triangleq \begin{cases} f_{p_1}^{-1}(x), & x \in F(H_1(p_1, p_2)), \\ f_{p_2}^{-1}(x), & x \in F(H_2(p_1, p_2)), \end{cases}$$

with $f_{p_1}^{-1}$ and $f_{p_2}^{-1}$ continuous on $H_1(p_1, p_2)$ and $H_2(p_1, p_2)$, respectively. It suffices to show that F^{-1} is well defined for $x \in F(H_1(p_1, p_2)) \cap F(H_2(p_1, p_2)) = F(\chi(p_1, p_2))$. To this end, notice that the statement $x \in F(\chi(p_1, p_2))$ implies that there exists $X \in \chi(p_1, p_2)$ such that $x = F(X)$. But $X \in \chi(p_1, p_2)$ implies that $|X - p_1| = |X - p_2|$ and hence $x = f_{p_1}(X) = f_{p_2}(X)$. It follows that $f_{p_1}^{-1}(x) = f_{p_2}^{-1}(x)$ for all $x \in F(\chi(p_1, p_2))$.

- vi) Since $p_1 \in \text{int}(H_1(p_1, p_2))$ [$p_2 \in \text{int}(H_2(p_1, p_2))$] and the restriction of F on $\text{int}(H_1(p_1, p_2))$ [$\text{int}(H_2(p_1, p_2))$] yields an open map, it follows that $p_1 = F(p_1) \in F(\text{int}(H_1(p_1, p_2))) \subset \text{int}(F(H_1(p_1, p_2)))$ [$p_2 \in \text{int}(F(H_2(p_1, p_2)))$].
- vii) Let us assume, on the contrary, that there exists $x \in \text{int}(F(H_1(p_1, p_2)))$ such that $c(x, p_1) \geq c(x, p_2)$. Let $X \in H_1(p_1, p_2)$ such $x = F(X)$. Note that iii) implies that $X \in \text{int}(H_1(p_1, p_2))$. It follows from Proposition 4 that $|X - p_1| \geq |X - p_2|$, contradicting the fact that $X \in \text{int}(H_1(p_1, p_2))$.
- viii) The proof follows from iii), vii) and Proposition 4. ■

So far we have solved the ZVDP for the case of two Voronoi generators and of a wind velocity field that varies uniformly with time. We are now ready to state the main theorem of this paper.

Theorem 1: Let $V \triangleq \{V_i, i \in \mathcal{I}\}$ be the standard Voronoi partition for the set of Voronoi generators $P \triangleq \{p_i, i \in \mathcal{I}\}$. Assume that $|w(t)| < 1$ for all $t \geq 0$, and let the function $F : \mathbb{R}^2 \mapsto \mathbb{R}^2$ be defined by

$$F = f_{p_i}(X), \quad X \in V_i, \quad i \in \mathcal{I}, \quad (17)$$

where $f_{p_i}(X) = X - \int_0^{d(X, p_i)} w(\tau) d\tau$, for $i \in \mathcal{I}$. The solution of the ZVDP is the image of V under the mapping F .

Proof: The Dirichlet domain V_i of the standard Voronoi partition V is determined by $V_i = \bigcap_{j \neq i} H_i(p_i, p_j)$ [4]. Thus, $F(V_i) = F(\bigcap_{j \neq i} H_i(p_i, p_j))$, which implies, by virtue of F being injective (Proposition 5v)), that $F(V_i) = \bigcap_{j \neq i} F(H_i(p_i, p_j))$. The proof can be carried out similarly to Proposition 5 using induction. ■

V. THE DUAL ZERMELO-VORONOI DIAGRAM

In this Section, driven by the observation that the minimum-time “distance” function is in general non-symmetric, that is, the minimum time to drive the system (1) from a point A to B, and vice versa, are not necessarily equal, we formulate a variation of the ZVDP. In particular, given a set of n agents starting from given initial positions, we want to characterize the set of terminal positions for each agent $i \in \{1, \dots, n\}$, denoted as \mathfrak{V}_i , such that every point in the interior of \mathfrak{V}_i can be reached by the agent i faster

than any other agent j , with $j \neq i$. We call this problem the Dual Zermelo-Voronoi Diagram Problem (DZVDP).

The distance function for the DZVDP is defined by

$$\tilde{c}(p_i, x_f) \triangleq T_f(p_i, x_f), \quad (18)$$

that is, the minimum time for the Zermelo navigation problem from a Voronoi generator p_i to the agent’s terminal configuration x_f . The generalized distance function for the DZVDP can be reduced to the distance function for the ZVDP by reversing the order of the function arguments. The construction of the DZVD is thus similar to the solution of the ZVD.

Corollary 1: Let $V \triangleq \{V_i, i \in \mathcal{I}\}$ be the standard Voronoi partition for the set of Voronoi generators $P \triangleq \{p_i, i \in \mathcal{I}\}$. Assume that $|w(t)| < 1$ for all $t \geq 0$, and let the function $\tilde{F} : \mathbb{R}^2 \mapsto \mathbb{R}^2$ be defined by

$$\tilde{F}(X) \triangleq \tilde{f}_{p_i}(X), \quad X \in V_i, \quad i \in \mathcal{I}, \quad (19)$$

where $\tilde{f}_{p_i}(X) \triangleq X + \int_0^{d(X, p_i)} w(\tau) d\tau$, $i \in \mathcal{I}$. The solution of the DZVDP is the image of V under the mapping \tilde{F} .

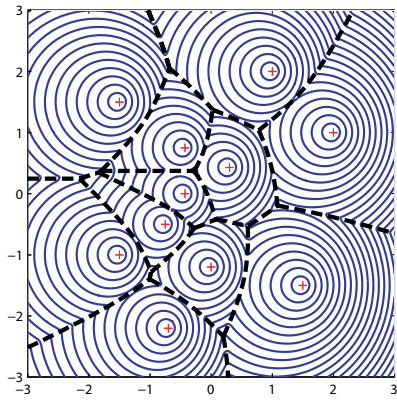
VI. SIMULATION RESULTS

In this section we provide numerical simulations to demonstrate the previous developments. To this end, let us consider the wind velocity field defined by

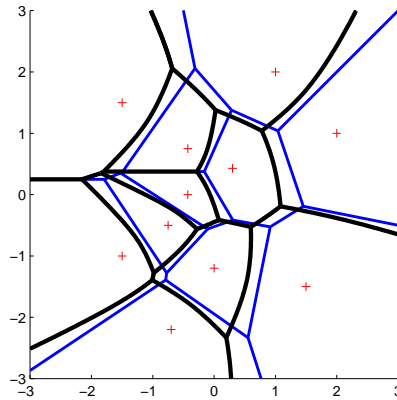
$$w(t) = \begin{cases} \bar{w} + \rho t, & 0 \leq t \leq \bar{t}, \\ \bar{w} + \rho \bar{t}, & t > \bar{t}, \end{cases} \quad (20)$$

where $\bar{w} = (\mu, \nu)^T \in \mathbb{R}^2$ with $|\bar{w}| < 1$, $\rho \in \mathbb{R}^2$ constants, and $\bar{t} < (1 - |\bar{w}|)/|\rho|$. We first construct the Zermelo-Voronoi Diagram by gridding the entire space and propagating the isocost fronts of the respective min-time problems emanating from each generator and we compare the results with the proposed approach in terms of computational efficiency. In particular, given a Voronoi generator $p \in P$, we define the minimum cost-to-go from x to p to be the function $K_p(x) \triangleq c(x, p)$. Next, we define the minimum cost-to-go to the set P as $K_P(x) = \min_{p \in P} c(x, p)$. Each Dirichlet domain of the ZVD can be determined by projecting the intersection of the surfaces K_P and K_p onto \mathfrak{X} . This method can be implemented by means of a fast marching algorithm, giving an approximation of the ZVD with time complexity $\mathcal{O}(NM \log M)$, where N is the number of elements of P , and M is the number of nodes of a grid that discretizes \mathfrak{X} [14] (note that M should be at least of order N^η , with $\eta > 1$). Figure 3(a) illustrates the ZVD specified by the previous exhaustive numerical method for $\bar{w} = (-0.3, 0.2)$ and $\rho = (0.05, -0.1)$ and a set of eleven Voronoi generators.

Next, we apply the approach introduced in this paper. In particular, we first construct the standard Voronoi Diagram of the set P , and then apply Theorem 1 to obtain the ZVD. Note that the construction of the standard Voronoi Diagram requires $\mathcal{O}(N \log N)$ time by using, for example, Fortune’s algorithm [17]. The mapping of the standard



(a) The ZVD and the minimum cost-to-go interpretation.



(b) The ZVD (black) and its corresponding standard Voronoi Diagram (blue).

Fig. 3. The exhaustive numerical and the efficient schemes for the construction of the Zermelo-Voronoi Diagram for a time-varying wind velocity field.

Voronoi Diagram, which consists of $\mathcal{O}(N)$ edges, to the ZVD requires $\mathcal{O}(N)$ time, giving a total time complexity for the construction of the ZVD which is of order $N \log N$. Figure 3(b) illustrates the ZVD we obtain after applying the transformation of Theorem 1 to the standard Voronoi Diagram.

Figure 4 illustrates the ZVD and the DZVD for the wind velocity field $w(t) = (0.5 + 0.1 \sin(t/\pi), -0.35 - 0.1 \cos(t/\pi))$. It is interesting to note that, as the wind becomes stronger, the Voronoi generators move closer to the boundaries of their corresponding Dirichlet domains, a pattern which is in accordance to the observations in [11].

VII. CONCLUSION

In this work we have addressed a generalized Voronoi Diagram, namely the Zermelo-Voronoi Diagram. In particular, we have dealt with the partition problem for a small airplane traveling in the horizontal plane in the presence of winds. Based on the interpretation of the Zermelo's problem as a moving target problem, we have shown that in case of a wind velocity field that varies uniformly with time,

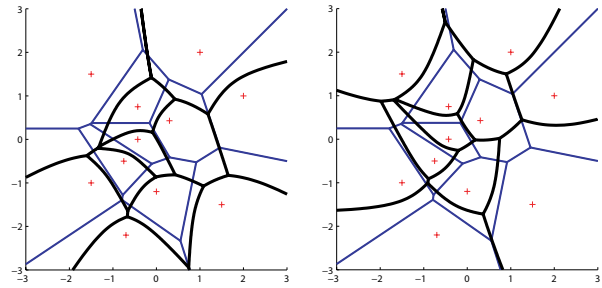


Fig. 4. The Zermelo Voronoi Diagram for a time-varying wind velocity field and a set of eleven Voronoi generators as constructed by means of a particular homeomorphism applied to the standard Voronoi diagram of the same set of generators.

the construction of the Zermelo-Voronoi Diagram can be associated with a standard Voronoi Diagram by means of a state transformation.

Acknowledgement: This work has been supported in part by NASA (award no. NNX08AB94A). The first author also acknowledges support from the A. Onassis Public Benefit Foundation.

REFERENCES

- [1] G. L. Dirichlet, "Über die Reduktion der Positiven Quadratischen Formen mit drei Unbestimmten Ganzen Zahlen," *Journal für die Reine und Angewandte Mathematik*, vol. 40, pp. 209 – 227, 1850.
- [2] G. F. Voronoi, "Nouvelles applications des paramètres continus à la théorie de formes quadratiques," *Journal für die Reine und Angewandte Mathematik*, vol. 134, pp. 198 – 287, 1908.
- [3] J.-D. Boissonnat, "Geometric structures for three-dimensional shape representation," *ACM Transactions on Graphics*, vol. 3, no. 4, pp. 266 – 286, 1984.
- [4] J. Gallier, *Geometric Methods and Applications: for Computer Science and Engineering*. New York, USA: Springer-Verlag, 2000.
- [5] S. M. Lavalle, *Planning Algorithms*. New York, NY: Cambridge University Press, 2006.
- [6] J. Cortés, S. Martínez, T. Karatas, and F. Bullo, "Coverage control for mobile sensing networks," *IEEE Transactions on Robotics and Automation*, vol. 20, no. 2, pp. 243 – 255, 2004.
- [7] J. Cortés and F. Bullo, "Coordination and geometric optimization via distributed dynamical systems," *SIAM Journal of Optimization and Control*, vol. 44, no. 5, pp. 1543 – 1574, 2005.
- [8] A. Okabe, B. Boots, K. Sugihara, and S. N. Chiu, *Spatial Tessellations: Concepts and Applications of Voronoi Diagrams*. West Sussex, England: John Wiley and Sons Ltd, second ed., 2000.
- [9] F. Aurenhammer, "Voronoi diagrams: A survey of a fundamental geometric data structure," *ACM Computing Surveys*, vol. 23, no. 3, pp. 345 – 405, 1991.
- [10] E. Zermelo, "Über das Navigationsproblem bei Ruhender oder Veränderlicher Windverteilung," *Z. Angew. Math. und. Mech.*, no. 11, 1931.
- [11] K. Sugihara, "Voronoi diagrams in a river," *International Journal of Computational Geometry and Applications*, vol. 2, pp. 29 – 48, 1992.
- [12] H. J. Kelley, "Guidance theory and extremal fields," *IRE Transactions on Automatic Control*, vol. AC-7, pp. 75 – 82, October 1962.
- [13] T. Nishida and K. Sugihara, "Voronoi diagram in the flow field," *Lecture Notes in Computer Science*, vol. 2906/2003, pp. 26 – 35, 2004.
- [14] T. Nishida, K. Sugihara, and M. Kimura, "Stable marker-particle method for the voronoi diagram in a flow field," *Journal of Computational and Applied Mathematics*, vol. 202, no. 2, pp. 377 – 391, 2007.
- [15] M. Cesari, *Optimization - Theory and Applications. Problems with Ordinary Differential Equations*. New York: Springer-Verlag, 1983.
- [16] C. Carathéodory, *Calculus of Variations and Partial Differential Equations of First Order*. Washington DC: American Mathematical Society, 3 ed., 1999.
- [17] S. Fortune, "A sweepline algorithm for Voronoi diagrams," *Algorithmica*, vol. 2, no. 1-4, pp. 153 – 174, 1987.